TUDelft

Delft University of Technology

A tour of Marchenko redatuming

Focusing the subsurface wavefield

Cui, Tianci; Vasconcelos, Ivan; Manen, Dirk Jan Van; Wapenaar, Kees

Important note
To cite this publication, please use the final published version (if applicable).
Please check the document version above.

A tour of Marchenko redatuming: Focusing the subsurface wavefield

Tianci Cui[1,3], Ivan Vasconcelos[2], Dirk-Jan van Manen[3], and Kees Wapenaar[4]

Abstract

Marchenko redatuming can retrieve the impulse response to a subsurface virtual source from the single-sided surface reflection data with limited knowledge of the medium. We illustrate the concepts and practical aspects of Marchenko redatuming on a simple 1D acoustic lossless medium in which the coupled Marchenko equations are exact. Defined in a truncated version of the actual medium, the Marchenko focusing functions focus the wavefields at the virtual source location and are responsible for the subsequent retrieval of the downgoing and upgoing components of the medium's impulse response. In real seismic exploration, where we have no access to the truncated medium, we solve the coupled Marchenko equations by iterative substitution, relying on the causality relations between the focusing functions and the desired Green's functions along with an initial estimate of the downgoing focusing function. We show that the amplitude accuracy of the initial focusing function influences that of the retrieved Green's functions. During each iteration, propagating an updated focusing function into the actual medium can be approximated by explicit convolution with the broadband reflection seismic data after appropriate processing, which acts as a proxy for the true medium's reflection response.

Introduction

Recent research on data-driven single-sided focusing, also known as Marchenko redatuming, has shown that the Green's response to a subsurface virtual source can be retrieved from single-sided surface reflection measurements. Superior to conventional redatuming methods, Marchenko redatuming has the potential to correctly retrieve all orders of internal multiples and to achieve target-oriented imaging, free of spurious events. The 1D Marchenko equation is well known in inverse scattering problems. Broggini and Snieder (2012) show that, going beyond seismic interferometry, Marchenko redatuming succeeds with single-sided illumination only, without requiring physical subsurface receivers. Based on the reciprocity theorems for one-way wavefields, Wapenaar et al. (2013) and Slob et al. (2014) derive 3D Marchenko equations, valid for lossless acoustic inhomogeneous media. van der Neut et al. (2015a) illustrate how the redatumed Green's function can be retrieved by iterative substitution of the coupled Marchenko equations, with limited knowledge of the medium, together with the surface reflection data and an estimate of the direct arrival of the inverse transmission response. Ongoing research has extended the theory and application of Marchenko redatuming to elastodynamic media (e.g., da Costa Filho et al., 2014; Wapenaar and Slob, 2014), complex media (Vasconcelos et al., 2014, 2015; Vasconcelos and van der Neut, 2016), dissipative media (Slob, 2016), and for data including free-surface multiples (e.g., Singh et al., 2015; Staring et al., 2016).

This tutorial works through a synthetic example for a 1D acoustic lossless medium without a free surface, where the Marchenko equation is exact. The theory of Marchenko redatuming is introduced at an intuitive level to illustrate the physics behind it. We discuss the implementation of Marchenko redatuming in the context of seismic exploration.

1D acoustic medium and the recorded wavefields

A 1D acoustic medium with three reflectors is modeled for which the wave propagation velocity and mass density vary with depth as shown in Figure 1a. We define this actual medium as "state B" while "state A" in Figure 1b is its truncated version, which is the same as the actual medium above the desired focusing datum at 300 m, indicated by a virtual source (hollow stars in Figure 1), and is reflection-free below it. In conventional seismic acquisition, a surface
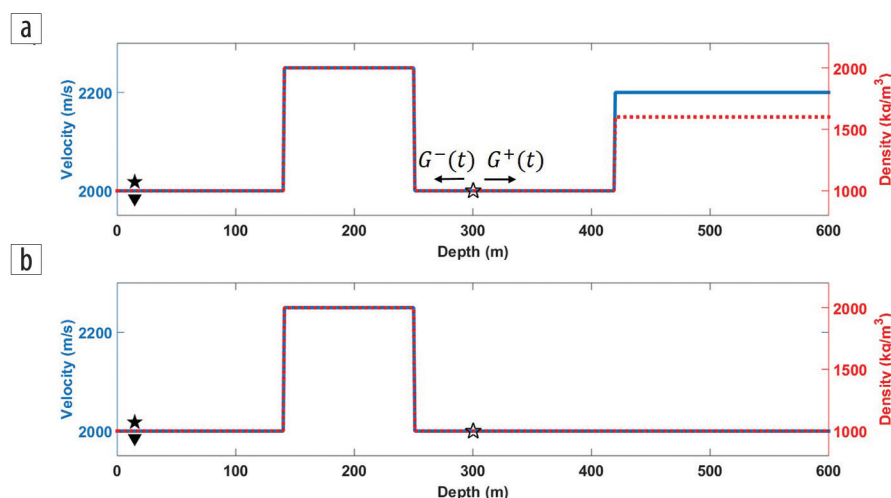
Figure 1. (a) State B: actual medium with underburden. (b) State A: truncated medium without underburden.

---

[1]Schlumberger Gould Research.
[2]Formerly Schlumberger Gould Research; presently Department of Earth Sciences, Utrecht University.
[3]Institute of Geophysics, ETH Zürich.
[4]Department of Geoscience and Engineering, Delft University of Technology.

geophone (solid triangles in Figure 1) records the reflection response to a surface source (solid stars in Figure 1). Seismic source redatuming aims at retrieving the response to a subsurface virtual source, recorded by the surface geophone.

Assuming that the medium is lossless and that there are no free-surface multiples, we model the reflection and transmission responses with the finite difference method. Figure 2 shows the recorded wavefields by igniting a Gaussian-shaped, zero-phase wavelet into the actual and truncated medium, respectively. Note that in state A, the transmission response $T(t)$ is the response of the medium between the subsurface virtual source and the surface receiver, whereas in state B, the transmission response $G(t)$ includes the response of the medium below the subsurface virtual source. In an idealized scenario, where the transmission response $T(t)$ and reflection response $R_A(t)$ of the truncated medium were assumed to be known, the transmission response $G(t)$ could be retrieved directly from the single-sided reflection response $R(t)$ of the actual medium, using the coupled Marchenko equations. We will discuss an iterative Marchenko scheme to retrieve $G(t)$ in a practical case where we have no access to the truncated medium information. As indicated by Figure 1a, the desired transmission response $G(t)$ — i.e., the total redatumed Green's function — consists of the downgoing Green's function $G^+(t)$ and the upgoing Green's function $G^-(t)$, and they can be retrieved separately. Note that the + and – signs used here indicate the propagation directions at the virtual source, which are opposite to common notations, which use these signs to indicate the propagation directions observed at a virtual receiver.

The coupled Marchenko equations

Wapenaar et al. (2013) and Slob et al. (2014) introduce the so-called focusing functions $f_1^+(t)$ and $f_1^-(t)$ in Marchenko redatuming based on state A. As defined by time-domain equations 1 and 2, the downgoing focusing function $f_1^+(t)$ is the inverse of the transmission response in the truncated medium, and its reflection response in the truncated medium is the upgoing focusing function $f_1^-(t)$,

$$T(t) * f_1^+(t) = \delta(t) \tag{1}$$

$$R_A(t) * f_1^+(t) = f_1^-(t), \tag{2}$$

where the asterisk indicates convolution. Here, both focusing functions $f_1^\pm(t)$ are essentially the focusing wavefields observed at the surface. Figure 3 shows the focusing functions calculated
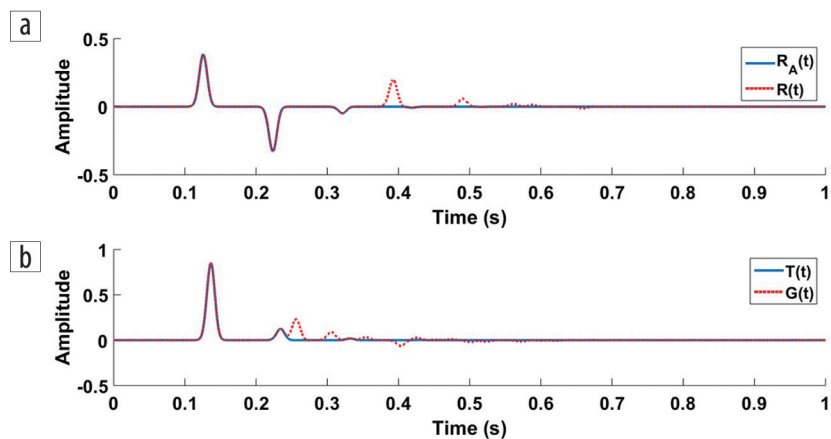

Figure 2. (a) Reflection responses of the truncated medium $R_A(t)$ and the actual medium $R(t)$. (b) Transmission responses of the truncated medium $T(t)$ and the actual medium $G(t)$.
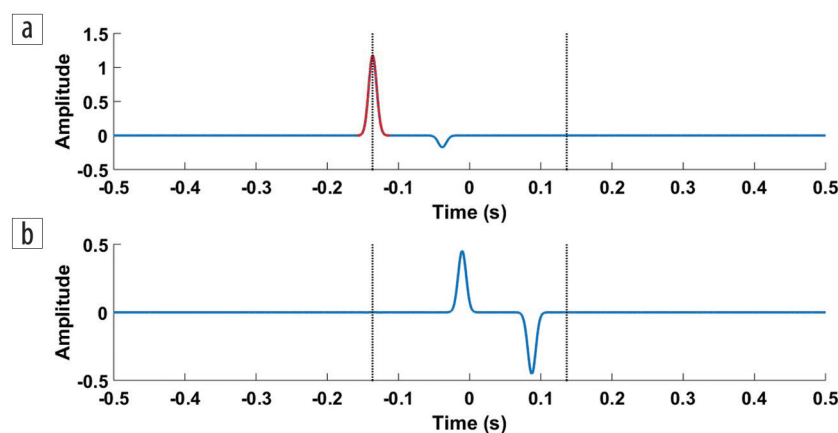

Figure 3. (a) Downgoing focusing function $f_1^+(t)$. (b) Upgoing focusing function $f_1^-(t)$. The vertical dotted lines denote the transmitted direct arrival time t_d and its time reversal $-t_d$.

directly from the transmission and reflection responses of the truncated medium in Figure 2. We later discuss how they can be retrieved from the reflection response of the actual medium.

Derived from the reciprocity theorems for one-way wavefields, the time-domain coupled Marchenko equations 3 and 4 directly relate the surface reflection response to the desired Green's functions in state B via the focusing functions defined in state A,

$$G^+(t) = R(t) * f_1^+(t) - f_1^-(t) \tag{3}$$

$$G^-(t) = -R(t) * f_1^-(-t) + f_1^+(-t). \tag{4}$$

Figures 4a and 4b are the downgoing and upgoing Green's functions, calculated once knowing the focusing functions. Their sum (Figure 4c, dotted red) is the total retrieved Green's function, which matches the surface recorded transmission response to a real source at the focusing datum in the actual medium (Figure 4c, solid blue), thus verifying the coupled Marchenko equations.

Figures 5 and 6 display the wavefields and space-time propagation diagrams associated with the Marchenko system, to physically interpret the coupled Marchenko equations. All of the wavefields are expressed in pressure on the same gray scale, where white and black indicate the positive and negative pressure values, respectively.

On top of the propagation diagrams are the corresponding traces being injected into the medium. The traveltime of the transmitted direct arrival from the focusing datum to the acquisition surface is denoted as t_d. In Figure 5a, injecting the shifted seismic wavelet at $-t_d$ (solid red) into the truncated medium will generate the upgoing primary reflections (dashed blue) as well as the undesired downgoing coda (dotted red), which reaches the focusing datum. In Figure 5b, the focusing function $f_1^+(t)$ (solid and dashed red) is injected into the truncated medium from time $-t_d$ onwards. Its coda $f_{1m}^+(t)$ (dashed red) propagates and meets the upgoing primary reflection (dashed blue; which is defined as $f_1^-(t)$ by equation 2 at each corresponding depth) to cancel the subsequent downgoing coda as in Figure 5a. As a result, the direct arrival $f_{1d}^+(t)$ (solid red) is focused at the focusing datum and at time zero. This focusing process is defined by equation 1. In the actual medium, the focused event acts as a pure downgoing virtual source (hollow star) to generate the wavefield associated with $G^+(t)$, which is described by Marchenko equation 3 and is shown in Figure 5c.

As is predicted by Marchenko equation 4 and shown by Figure 6a, injecting the time-reversed focusing function $f_1^-(-t)$ (dashed blue) into the actual medium generates the time-reversed focusing function $f_1^+(-t)$ (dashed and solid red). The subsequent waves propagate as if there is a pure upgoing virtual source (reverse polarity compared to the downgoing virtual source) at the focusing datum and at time zero indicated by a hollow star (the interception between the focusing datum and the elongated $f_{1d}^+(-t)$ in dotted red). This generates the wavefield associated with $-G^-(t)$, whose direct arrival $-G_d^-(t)$ overlaps with $f_{1d}^+(-t)$ (solid red). The wavefield $G^-(t)$ generated from a real source (solid star) is displayed in Figure 6b with reverse polarity. It is computed by subtracting the wavefield $G^+(t)$ in Figure 5c from the total wavefield $G(t)$, which, in turn, is modeled by igniting a real source located at the focusing datum and at time zero. Subtracting Figure 6b from Figure 6a, Figure 6c shows that their wavefields are the same
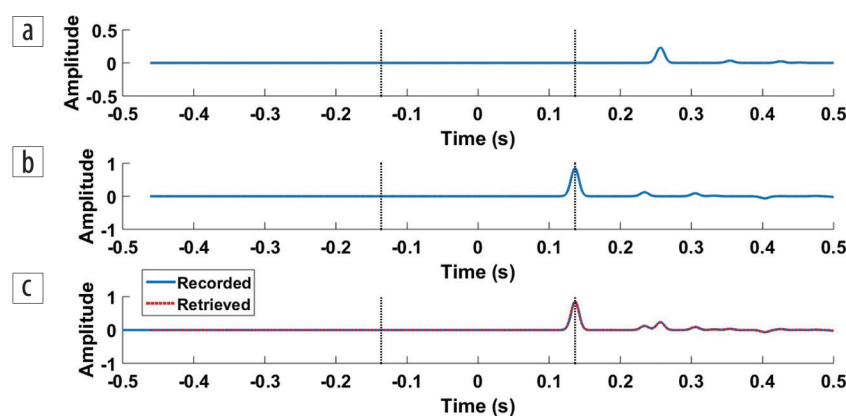

Figure 4. (a) Downgoing Green's function $G^+(t)$. (b) Upgoing Green's function $G^-(t)$. (c) Total Green's functions by direct modeling and Marchenko redatuming. The vertical dotted lines denote the transmitted direct arrival time t_d and its time reversal $-t_d$.
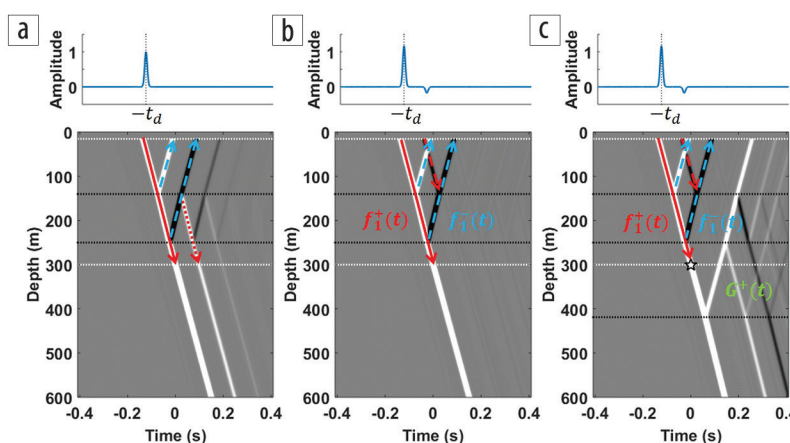

Figure 5. Wavefields of (a) injecting the source wavelet at $-t_d$ into the truncated medium, (b) injecting the focusing function $f_1^+(t)$ into the truncated medium, (c) injecting the focusing function $f_1^+(t)$ into the actual medium where the hollow star indicates the virtual source location. The horizontal dotted lines in each figure denote specific depth levels: the black are the reflectors, the white are the acquisition surface and the focusing datum from top to bottom.

Figure 6. Wavefields of (a) injecting the focusing function $f_1^-(-t)$ into the actual medium where the hollow star denotes the virtual source location, (b) $-G^-(t)$ modeled with a real subsurface source indicated by a solid star. The solid red ray indicates the direct arrival of the Green's function $-G_d^-(t)$. (c) Difference between Figures 6a and 6b. The horizontal dotted lines in each figure denote specific depth levels: the black are the reflectors, the white are the acquisition surface and the focusing datum from top to bottom.
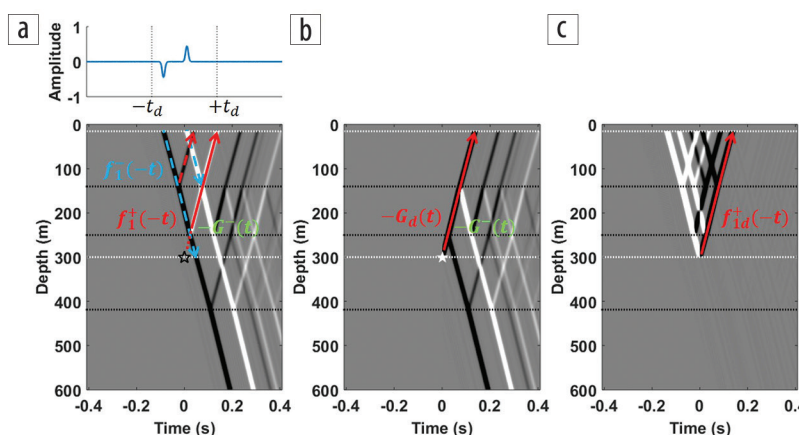
following the direct arrival $f_{1d}^+(-t)$ (solid red), verifying that the wavefield $G^-(t)$ is generated as described by Marchenko

equation 4, although the subsurface source is not physically formed.

The iterative Marchenko scheme

In practice, seismic acquisition obtains the reflection response of the actual medium, where no information about the truncated medium is available a priori and neither are the focusing functions. However, it is possible to solve the underdetermined coupled Marchenko equations because of the causality properties of the focusing functions and the desired Green's functions. In this tutorial, we rely on an iterative scheme (e.g., van der Neut et al., 2015a), although other approaches such as direct inversion are also available.

To capture the causality of the focusing functions and the desired Green's functions, a windowing operator $\theta\{\cdot\}$ is introduced. This operator is designed to remove all the events arriving at and after t_d as well as all the acausal events at and before $-t_d$. The timing of the direct arrival and its time reversal is denoted by the vertical dotted lines in Figures 3 and 4. As is seen from Figure 3a, the downgoing focusing function is composed by its direct arrival (dotted red) at $-t_d$ and a following coda between $-t_d$ and t_d. Applying the windowing operation to the downgoing focusing function gives

$$\theta\{f_1^+(t)\} = \theta\{f_{1d}^+(t) + f_{1m}^+(t)\} = f_{1m}^+(t) . \qquad (5)$$

Figure 3b shows that the upgoing focusing function $f_1^-(t)$ arrives between $-t_d$ and t_d so that

$$\theta\{f_1^-(t)\} = f_1^-(t) . \qquad (6)$$

Because of causality, all the events of the Green's functions appear at or after t_d (Figure 4) such that

$$\theta\{G^+(t)\} = 0 , \qquad (7)$$

and

$$\theta\{G^-(t)\} = 0 . \qquad (8)$$

Thus, the coupled Marchenko equations 3 and 4 after the windowing operation on both sides become

$$\theta\{R(t)*[f_{1d}^+(t) + f_{1m}^+(t)]\} = f_1^-(t) , \qquad (9)$$

and

Figure 7. Focusing function $f_1^+(t)$ updates of (a) the first and (b) third iterations compared to the one calculated from the known $T(t)$ in Figure 3a. The vertical dotted lines denote the transmitted direct arrival time t_d and its time reversal $-t_d$. (c) Difference of the estimated $f_1^+(t)$ between the third and fourth iterations.

Figure 8. Focusing function $f_1^-(t)$ updates of (a) the first and (b) third iterations compared to the one calculated from the known $T(t)$ and $R_A(t)$ in Figure 3b. The vertical dotted lines denote the transmitted direct arrival time t_d and its time reversal $-t_d$. (c) Difference of the estimated $f_1^-(t)$ between the third and fourth iterations.

$$\theta\{R(t)*f_1^-(-t)\} = f_{1m}^+(-t) . \qquad (10)$$

With acquisition of the reflection response $R(t)$ and an estimate of the initial focusing function $f_{1d}^+(t)$, equations 9 and 10 can be solved by iterative substitution.

To start the iteration, the initial value of $f_{1m}^+(t)$ is assumed to be zero so that the first estimate of $f_1^-(t)$ can be obtained by equation 9 and then be inserted into equation 10 to update the value of $f_{1m}^+(t)$. During the second iteration, the estimate of $f_{1m}^+(t)$ from the first iteration is added to $f_{1d}^+(t)$ to get the second estimate of $f_1^-(t)$, update $f_{1m}^+(t)$ again, and proceed to the next iterations. Figures 7 and 8 show the focusing function updates of the first and third iterations, compared to the ones calculated from the known truncated medium responses. The difference of the estimates is invisible between the third and fourth iterations on the same scale as the corresponding focusing function plot, implying that the iterative Marchenko scheme converges after three iterations for this simple 1D acoustic medium.

In theory, the initial focusing function $f_{1d}^+(t)$ is the direct arrival of the inverse transmission response in the truncated medium. In practice, it is often approximated as the direct arrival of the
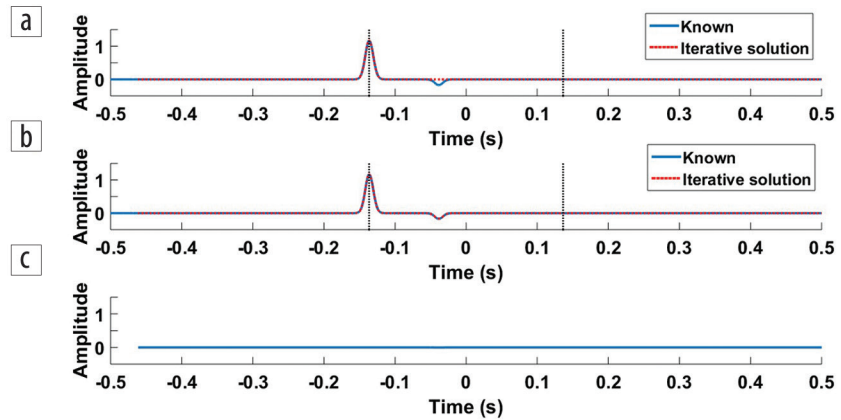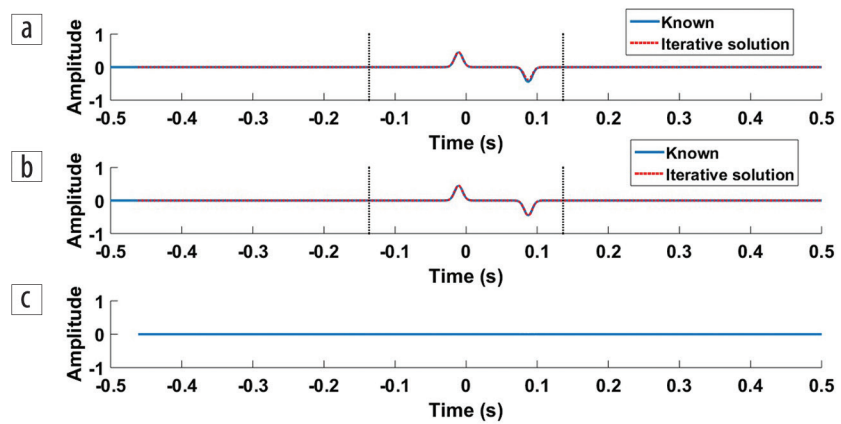
time-reversed transmission response, which can be computed in a reference macro-velocity model. As is shown in Figure 9a, the direct arrival of $T(-t)$ shares the traveltime with that of $T^{-1}(t)$, while its amplitude is incorrect, resulting in an overall amplitude error of the retrieved Green's function in Figure 9c.

The iterative Marchenko scheme by explicit data convolution

In the numerical example shown earlier, each iteration is conducted by propagating an updated focusing function or its time reversal into the real medium by means of numerical simulation. In that case, the convolutions with the reflectivity operator remain implicit in the process of injecting the corresponding wavefields into the medium, either physically or numerically. In practice, it is unrealistic to repeat the seismic acquisition many times so that each time a specific set of surface sources are designed to yield corresponding focusing functions. Instead, the operations involving $R(t)$ during each Marchenko iteration can be conducted using explicit convolution with recorded data: where $R(t)$ is no longer the true reflection response of the medium, but is taken from finite-time, finite-bandwidth reflection seismic data, after appropriate signal processing (e.g., source deconvolution, data regularization, and removal of direct arrivals and free-surface effects).

Assuming that the source wavelet to be deconvolved is unknown, blind deconvolution (e.g., Robinson and Treitel, 1980) is one of several possible approaches to estimate it from the data. Take the frequency-domain spiking deconvolution as an example. We estimate the amplitude spectrum of the source wavelet by smoothing that of the reflection response and assume that the wavelet phase is known to be zero. Because the estimated wavelet has the ambiguity of a scalar, the deconvolved reflection response needs to be correctly scaled so that the iterative Marchenko scheme converges. We scale the source wavelet estimated from the reflection response with respect to the known wavelet shown in Figure 10b. van der Neut et al. (2015b) and Brackenhoff (2016) further discuss the possibility of calculating the correct scaling factor in a realistic case where the source wavelet is unknown. Deconvolving this estimated wavelet from the reflection response gets a similar reflection estimate with a broader bandwidth as the deterministic deconvolution by knowing the wavelet shown in Figure 10c. Starting with the direct arrival of T^{-1} as the initial focusing function, the total Green's functions are properly retrieved by the iterative explicit convolution with the deconvolved reflection response from either the deterministic deconvolution or the blind deconvolution with
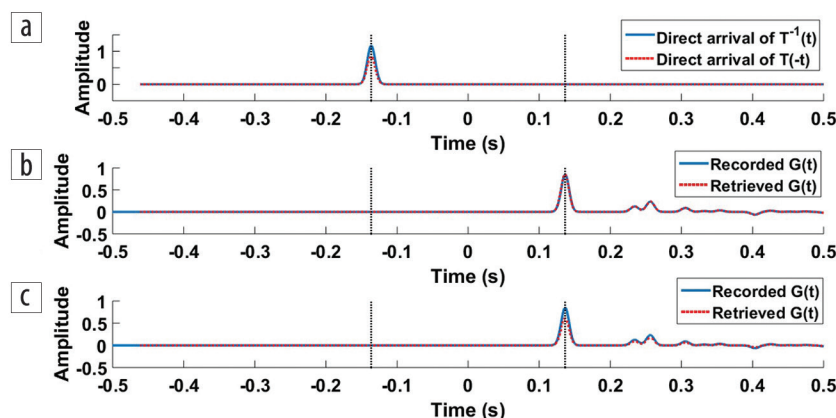

Figure 9. (a) Initial focusing functions: direct arrival of the inverse transmission response and direct arrival of the time-reversed transmission response in the truncated medium. (b) The total Green's function retrieved by Marchenko redatuming using the direct arrival of $T^{-1}(t)$ as the initial focusing function after three iterations compared to the one recorded from direct modeling. (c) The total Green's function retrieved by Marchenko redatuming using the direct arrival of $T(-t)$ as the initial focusing function after three iterations compared to the one recorded from direct modeling. The vertical dotted lines denote the transmitted direct arrival time t_d and its time reversal $-t_d$.
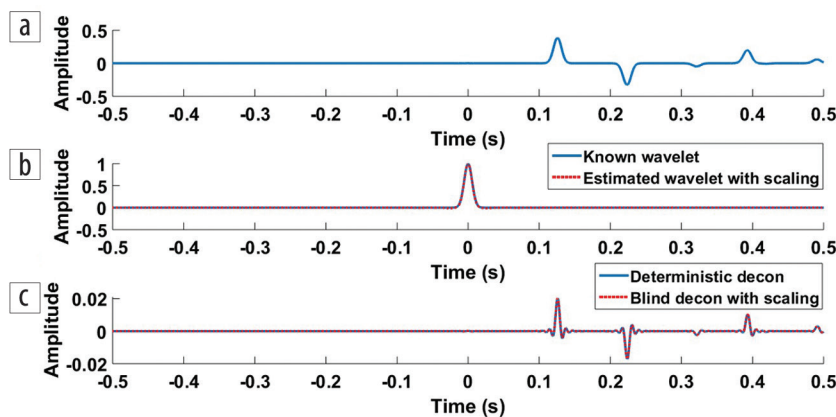

Figure 10. (a) Reflection response of the actual medium, same as the dotted red trace in Figure 2a. (b) The source wavelet estimated during the blind deconvolution followed by correct scaling compared to the known wavelet. (c) Deconvolved reflection response using the known source wavelet compared to that using the estimated wavelet followed by correct scaling.

correct scaling, although the latter has subtle amplitude errors as shown in Figure 11b.

Conclusions

In this tutorial, we illustrate Marchenko redatuming on a synthetic model of a 1D acoustic lossless medium. For the sake of discussion, by knowing its truncated version (not practical in real experiments), we can directly calculate the focusing functions. As described by the coupled Marchenko equations, the focusing functions focus the wavefield in the subsurface to get the impulse response to the subsurface virtual source. In the more realistic case where truncated medium information is not available, we can solve the coupled Marchenko equations by iterative substitution, based on the causality properties of the focusing functions and the desired Green's functions. With an estimate of the initial focusing function, the redatumed Green's functions can be retrieved from the single-sided surface reflection response. The amplitude error of the estimated initial focusing function influences the accuracy of the retrieved Green's functions. In seismic exploration, the iterative scheme can be

conducted by explicit convolution with the broadband reflection data after signal processing, acting as a proxy for the true medium's reflection response.

Going from 1D to 3D, acoustic to elastodynamic, and/or simple to complex media, the direct arrival of the time-reversed transmission response is less well-posed and thus harder to estimate. Whether its accuracy is sufficient to initialize the focusing function may vary on a case-by-case basis, where the degree of lateral heterogeneity and the acquisition design will likely be the controlling factors for the success of the scheme. With some initial success on field data (e.g., Ravasi et al., 2016), we believe the scheme is already practical in cases where data coverage is sufficient and medium lateral heterogeneity is moderate. Improving the initial focusing functions, the windowing operator design, and the method's applicability of handling unknown source wavelets, irregular acquisition geometries, attenuation, and complex media are topics of ongoing research for Marchenko redatuming. **TLE**

Figure 11. The Marchenko retrieved Green's functions by iterative explicit convolution with the broadband reflection response from (a) the deterministic deconvolution and (b) the blind deconvolution with correct scaling after three iterations, compared to the one recorded from direct modeling. The vertical dotted lines denote the transmitted direct arrival time t_d and its time reversal $-t_d$.

Acknowledgments

Corresponding author: tcui2@slb.com

References

Brackenhoff, J., 2016, Rescaling of incorrect source strength using Marchenko redatuming: MSc thesis, Delft University of Technology.

Broggini, F., and R. Snieder, 2012, Connection of scattering principles: A visual and mathematical tour: European Journal of Physics, **33**, no. 3, 593–613, https://doi.org/10.1088/0143-0807/33/3/593.

da Costa Filho, C. A., M. Ravasi, A. Curtis, and G. A. Meles, 2014, Elastodynamic Green's function retrieval through single-sided Marchenko inverse scattering: Physical Review, **90**, no. 6, https://doi.org/10.1103/PhysRevE.90.063201.

Ravasi, M., I. Vasconcelos, A. Kritski, A. Curtis, C. A. da Costa Filho, and G. A. Meles, 2016, Target-oriented Marchenko imaging of a North Sea field: Geophysical Journal International, **205**, no. 1, 99–104, https://doi.org/10.1093/gji/ggv528.

Robinson, E. A., and S. Treitel, 1980, Geophysical signal analysis: Prentice Hall Inc.

Singh, S., R. Snieder, J. Behura, J. van der Neut, K. Wapenaar, and E. Slob, 2015, Marchenko imaging: Imaging with primaries, internal multiples, and free-surface multiples: Geophysics, **80**, no. 5, S165–S174, https://doi.org/10.1190/geo2014-0494.1.

Slob, E., 2016, Green's function retrieval and Marchenko imaging in a dissipative acoustic medium: Physical Review Letters, **116**, no. 16, https://doi.org/10.1103/PhysRevLett.116.164301.

Slob, E., K. Wapenaar, F. Broggini, and R. Snieder, 2014, Seismic reflector imaging using internal multiples with Marchenko-type equations: Geophysics, **79**, no. 2, S63–S76, https://doi.org/10.1190/geo2013-0095.1.

Staring, M., J. van der Neut, and C. Wapenaar, 2016, An interferometric interpretation of Marchenko redatuming including free-surface multiples: 86th Annual International Meeting, SEG, Expanded Abstracts, 5172–5176, https://doi.org/10.1190/segam2016-13956290.1.

van der Neut, J., I. Vasconcelos, and K. Wapenaar, 2015a, On Green's function retrieval by iterative substitution of the coupled Marchenko equations: Geophysical Journal International, **203**, no. 2, 792–813, https://doi.org/10.1093/gji/ggv330.

van der Neut, J., K. Wapenaar, J. Thorbecke, and E. Slob, 2015b, Practical challenges in adaptive Marchenko imaging: 85th Annual International Meeting, SEG, Expanded Abstracts, 4505–4509, https://doi.org/10.1190/segam2015-5791035.1.

Vasconcelos, I., and J. van der Neut, 2016, Full-wavefield redatuming of perturbed fields with the Marchenko method: 78th Annual International Conference and Exhibition, EAGE, Extended Abstracts.

Vasconcelos, I., D. J. van Manen, M. Ravasi, K. Wapenaar, and J. van der Neut, 2014, Marchenko redatuming: Advantages and limitations in complex media, http://geodus1.ta.tudelft.nl/PrivatePages/C.P.A.Wapenaar/6_Proceedings/Soc.Expl.Geoph/Seg_14d.pdf, accessed 28 July 2017.

Vasconcelos, I., K. Wapenaar, J. van der Neut, C. Thomson, and M. Ravasi, 2015, Using inverse transmission matrices for Marchenko redatuming in highly complex media: 85th Annual International Meeting, SEG, Expanded Abstracts, 5081–5086, https://doi.org/10.1190/segam2015-5896301.1.

Wapenaar, K., and E. Slob, 2014, On the Marchenko equation for multicomponent single-sided reflection data: Geophysical Journal International, **199**, no. 3, 1367–1371, https://doi.org/10.1093/gji/ggu313.

Wapenaar, K., F. Broggini, E. Slob, and R. Snieder, 2013, Three-dimensional single-sided Marchenko inverse scattering, data-driven focusing, Green's function retrieval, and their mutual relations: Physical Review Letters, **110**, no. 8, htt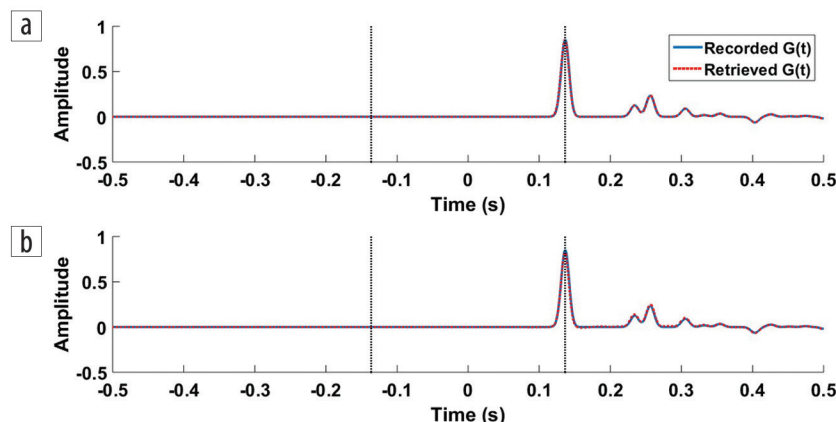ps://doi.org/10.1103/PhysRevLett.110.084301.